sibility that among the various types of antibodies present in the polyclonal sera some will be able to bind to their target regardless of the exact state in which the HMG is found in the cell. Indeed, using microinjection techniques we have found that the anti-HMG-1 antibody can bind to the antigen under in vivo conditions (L. Einck and M. Bustin, unpublished results). Thus it is feasible that microinjection of functional antibodies will help elucidate the cellular role of these proteins.

Acknowledgments

We thank Delores Proctor for editorial assistance.

References

Baker, C., Isenberg, I., Goodwin, G. H., & Johns, E. W. (1976) *Biochemistry 15*, 1645–1649.
Bhullar, B. S., Hewitt, J., & Candido, E. P. M. (1981) *J. Biol. Chem. 256*, 8801–8806.
Bustin, M. (1979) *Curr. Top. Microbiol. Immunol. 88*, 105–142.
Bustin, M., & Neihart, N. K. (1979) *Cell (Cambridge, Mass.) 16*, 181–189.
Bustin, M., Hopkins, R. B., & Isenberg, I. (1977) *J. Biol. Chem. 252*, 1694–1699.
Bustin, M., Reisch, J., Einck, L., & Klippel, J. H. (1982) *Science (Washington, D.C.) 215*, 1245–1267.
Crumpton, M. J. (1974) in *The Antigens* (Sela, M., Ed.) Vol. II, p 15, Academic Press, New York.
Goodwin, G. H., & Johns, E. W. (1978) *Biochim. Biophy. Acta 519*, 279–284.
Goodwin, G. H., Shooter, K. V., & Johns, E. W. (1975) *Eur. J. Biochem. 54*, 427–433.
Javaherian, K., Liu, F. L., & Wang, J. C. (1978) *Science (Washington, D.C.) 199*, 1345–1346.
Kohler, G., & Milstein, C. (1977) *Nature (London) 256*, 495–497.
Kurth, P. D., & Bustin, M. (1981) *J. Cell Biol. 89*, 70–77.
LeStourgeon, W. M., & Rush, H. P. (1973) *Arch. Biochem. Biophys. 155*, 144–158.
Levy, B. W., Wang, N. C. W., & Dixon, G. H. (1977) *Proc. Natl. Acad. Sci. U.S.A. 74*, 2810–2814.
Renart, J., Reiser, J., & Stark, G. R. (1979) *Proc. Natl. Acad. Sci. U.S.A. 76*, 3116–3120.
Romani, R., Rodman, T. C., Vidalli, G., & Bustin, M. (1979) *J. Biol. Chem. 254*, 2918–2922.
Romani, M., Vidalli, G., Tahourdin, C. S. M., & Bustin, M. (1980) *J. Biol. Chem. 255*, 468–474.
Sela, M., Schechter, B., Schechter, I., & Borek, F. (1967) *Cold Spring Harbor Symp. Quant. Biol. 32*, 537–549.
Seyedin, S. M., & Kistler, W. S. (1979) *J. Biol. Chem. 254*, 11264–11271.
Shooter, K. V., Goodwin, G. H., & Johns, E. W. (1974) *Eur. J. Biochem. 47*, 263–270.
Smith, B. J., Robertson, D., Birbeck, M. S. C., Goodwin, G. H., & Johns, E. W. (1978) *Exp. Cell Res. 115*, 420–423.
Spiker, S., Mardian, J. K. W., & Isenberg, I. (1978) *Biochem. Biophys. Res. Commun. 82*, 125–129.
Sterner, R., Boffa, L. C., & Vidalli, G. (1978) *J. Biol. Chem. 253*, 3830–3836.
Vidali, G., Boffa, L. C., & Allfrey, V. G. (1977) *Cell (Cambridge, Mass.) 12*, 409–415.
Walker, T. M., Gooderham, K., Hastings, R. B., Mayes, E., & Johns, E. W. (1980) *FEBS Lett. 122*, 264–270.

Cobalt–Bleomycin–Deoxyribonucleic Acid System. Evidence of Deoxyribonucleic Acid Bound Superoxo and μ-Peroxo Cobalt–Bleomycin Complexes†

J. P. Albertini and A. Garnier-Suillerot*

ABSTRACT: Co(II) interacts with bleomycin in aqueous solution, in the presence of air, to give a short-lived mononuclear superoxo Co(III) complex (I). Then, two molecules of complex I react together, with the loss of oxygen, to yield the dinuclear μ-peroxo Co(III) complex (II); the dimerization follows a second-order rate law with $k_2 = 200 \pm 50$ M^{-1} s^{-1} at 25 °C. The rate of dimerization is lowered by a factor of 2000 when DNA is present at a molar ratio of [nucleotide]/[Co] higher than 16. These results and studies of circular dichroism and electron paramagnetic resonance spectra of complexes strongly suggest the binding of the superoxo complex to DNA (I′) as well as that of the μ-peroxo complex (II′); the binding of 1 molecule of complex II for every 2.9 base pairs in DNA has been determined with an apparent equilibrium constant of 8.4×10^4 M^{-1}.

Bleomycins (BLM) are a family of glycopeptide antibiotics clinically prescribed for the treatment of selected neoplasmic diseases (Carter, 1978). This drug, which both chelates metal ions and binds to deoxyribonucleic acid (DNA), induces a degradation of DNA in a reaction that has been shown to depend, in vitro, on the presence of ferrous ion and molecular oxygen (Sausville et al., 1978). BLM can form stable complexes with other metal ions such as Cu(II), Zn(II), and Co(III) (Dabrowiak, 1980). With the exception of the Co(III) complexes, all the others have antitumor properties against the Ehrlich ascites tumor (Rao et al., 1980). On the other hand, labeled metal-bleomycin complexes are used for diagnostic tumor localization, and the Co^{III}·BLM complex, the more stable of the M·BLM complexes, exhibits excellent tumor-localizing properties in man (Rasker et al., 1975).

† From the Laboratoire de Bioinorganique, U.E.R. de Santé, Médecine et Biologie Humanie, Université Paris XIII, 93012 Bobigny Cedex, France, and the Laboratoire Associé au CNRS No. 71, Département de Recherches Physiques, Université Pierre et Marie Curie, 75230 Paris Cedex 05, France. *Received June 18, 1982.*

0006-2960/82/0421-6777$01.25/0

Moreover, BLM·^{57}Co has been shown to be a good tumor scanning agent for the diagnosis of pulmonary and cerebral tumors (Kono et al., 1977). Thus it appears important to accurately characterize the complexes formed between BLM and cobalt.

In recent years, the interaction of Co(II) with BLM has been a subject of increasing interest (Sugiura, 1980; Tsukayama et al., 1981; Vos et al., 1980a,b; Kakinuma et al., 1980; DeRiemer et al., 1979). Sugiura, in particular, has shown, via electron paramagnetic resonance (EPR) measurements, that by addition of Co(II) to an aqueous solution of BLM, a low-spin cobalt complex, presumably BLM·Co^{III}·O_2^-, is formed (Sugiura, 1980). However, Vos et al. (1980a,b) were able to demonstrate that, under the conditions studied by Sugiura, there is, in fact, an equilibrium between two complexes. On the other hand, Kakinuma et al. (1980) pointed out that different kinds of Co·BLM complexes could be separated by silica gel thin-layer chromatography, and DeRiemer et al. (1979) showed that two compounds were obtained by mixing Co(II) with BLM: only one of them being thermodynamically stable.

These observations prompted us to initiate an investigation on the interaction of Co(II) with BLM in order to identify accurately the different species formed. In a short paper, we reported that in aqueous solution, in the presence of oxygen, Co(II) reacts with BLM to give BLM·Co^{III}·O_2^-, which dimerizes to a μ-peroxo complex that is the thermodynamically stable compound (Garnier-Suillerot et al., 1981). In addition, we showed that the superoxo complex is greatly stabilized by the presence of DNA.

In the present paper, we give the results of an investigation in which the superoxo and the μ-peroxo complexes that are formed either in the absence or in the presence of DNA are accurately identified. Moreover, we show that both complexes bind to DNA and that 1 molecule of μ-peroxo complex binds for every 2.9 base pairs in DNA. This is an important point as Co·BLM complex fixation is used for tumor localization.

This investigatioin was done essentially by absorption, circular dichroism (CD), and EPR measurements. Thermodynamic parameters were also determined.

Materials and Methods

Purified BLM A_2 which contains (3-aminopropyl)dimethylsulfonium [$-NH(CH_2)_3S^+(CH_3)_2$] at the terminal amine was kindly provided by Laboratoire Roger Bellon. Standard Co(II) solutions were prepared from reagent-grade material [$CoSO_4$, $(NH_4)_2SO_4 \cdot 6H_2O$]. Calf thymus DNA was purchased from Sigma Chemical Co. All other reagents were of the highest quality available, and deionized distilled water was used throughout the experiments. Unless otherwise stated, samples of oxygenated species were prepared directly by the reaction of the antibiotics and Co(II) salt in 0.01 M Hepes [*N*-(2-hydroxyethyl)piperazine-*N*′-2-ethanesulfonic acid] buffer, pH 7.4, in open air. The Co(II) and BLM concentrations used ranged from 100 to 400 μM, and for ensurance of complete complexation, the molar ratio of BLM to cobalt was always higher than 1.

Absorption spectra were recorded on a Cary 219 spectrophotometer; CD spectra on a Jobin Yvon dichrograph Model Mark III; EPR spectra on a Varian CSE 109 spectrophotometer at −180 °C. The O_2 concentration measurements were performed with a YSI 5331 oxygen probe.

Results and Discussion

The addition of Co(II) to an aqueous solution of BLM, in the presence of air, gives rise to the rapid formation of a brown complex (I), which evolves to a green one (II). The reaction I → II, which is fast at room temperature, becomes slow enough near 0 °C to allow an accurate study of complex I. Nevertheless, data must be collected rapidly as complex I, even at ice temperature, has a lifetime of only a few minutes.

Complex I: *BLM·Co^{III}·O_2^-*. The formation of complex I is attested by the appearance of a band at 470 nm in the visible absorption spectrum. The stoichiometry and the pH-dependent formation of this complex were determined by absorbancies at 470 nm as a function of the BLM/Co molar ratio at different pH values. Complex I is completely formed at pH 4 and remains unaltered from pH 4 to 10; the complex stoichiometry is then 1:1. Concomitantly with the appearance of the absorption band, 1 mol of O_2/Co(II) is consumed, and an EPR spectrum characteristic of Co(III)-bound superoxide is obtained (Sugiura, 1980). We determined the following EPR parameters: $g_\perp$, 2.007; $g_\parallel$, 2.096; $A_\perp^{Co}$, 12.5 G; $A_\parallel^{Co}$ 20.0 G. Complex I can be then formulated as BLM·Co^{III}·O_2^-.

Complex II: *$(BLM \cdot Co^{III})_2 \cdot (\mu\text{-}O_2^{2-})$*. The reaction I → II is characterized by the decrease of the absorption band at 470 nm, as time elapses, and the reaction can conveniently be followed by monitoring this band. The reaction is also characterized by the presence of an isosbestic point at 580 nm in the absorption spectra (Figure 1). Concomitantly with the decrease of the 470-nm absorption band, 1 mol of oxygen/2 mol of Co(III) is released, and the EPR signal disappears (Garnier-Suillerot et al., 1981). The absorbance at 470 nm and the O_2 consumption have been determined simultaneously, and as can be seen in Figure 1 (insert), the plot of ϵ/Co at 470 nm against Co/O_2 consumed is a straight line. Therefore, the stoichiometry of complex II is that of a dimeric dioxygen adduct. This, as well as the diamagnetism, strongly suggests a μ-peroxo dicobalt structure for II, and the reaction I → II can be unambiguously formulated as

$$2(\text{BLM}\cdot Co^{III}\cdot O_2^-) \rightarrow (\text{BLM}\cdot Co^{III})_2\cdot(\mu\text{-}O_2^{2-}) + O_2$$

This equilibrium is not unexpected as it is well-known that 1:1 superoxo complexes are generally fleeting intermediates on the way to bridging species (McLendon & Martell, 1976; Lever & Gray, 1978).

This reaction follows a second-order rate law, and the kinetics are independent of pH in the range 4–10. The value of the second-order rate constant has been determined at different temperatures: at 25 °C in Hepes buffer (0.01 M, pH 7.4), $K_2 = 200 \pm 50$ M^{-1}. By use of a least-squares fitting method, a value of 20 ± 5 kcal M^{-1} for the activation energy of this reaction has been determined.

Absorption and CD Spectra of Complexes I and II. The absorption and CD spectra of complexes I and II are shown in Figures 1 and 2 (curve A), respectively, and the data are collected in Table I. In the visible region, the absorption spectrum of complex II exhibits two bands that have intensities consistent with Laporte-forbidden, spin-allowed, transitions (Lever, 1968). The absorption spectrum of complex I exhibits only one asymmetrical band at 460 nm with a relatively high molar absorption coefficient (750) for a d–d transition; in fact, this might be accounted for by overlapping with a shoulder at 385 nm, the intensity of the band at 460 nm being comparable to that that occurs at the same wavelength in complex II. In the visible CD spectra of both complexes, only two bands are present; this strongly suggests that the site symmetry around to cobalt ion is high and that the spectra of the two complexes can be analyzed by using C_{4v} symmetry. In this point group the first excited electronic state of the low-spin d^6 ion splits into an $^1A_2$ and ^1E state; the band that appears in both complexes at about 460 nm can thus be assigned to

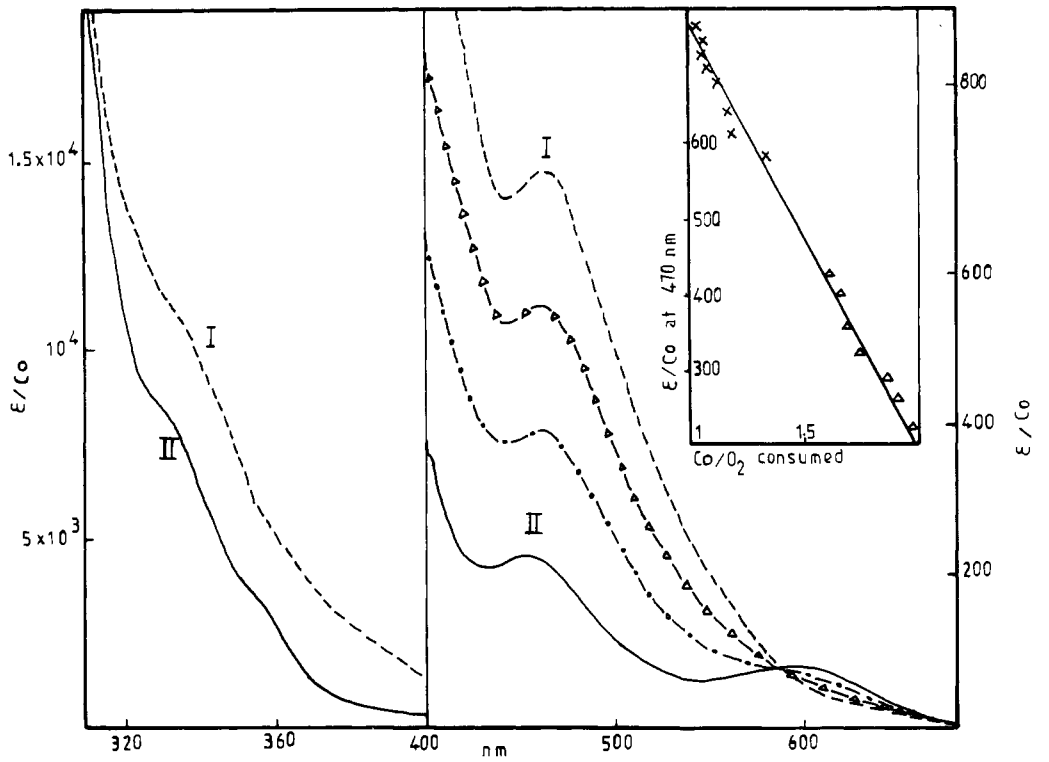

FIGURE 1: Absorption spectra of complex I (--) and complex II (—). The spectra have been recorded at various times after the addition of Co(II) to a BLM solution. Experimental conditions: 200 μM Co(II), 350 μM BLM in 0.01 M Hepes buffer, pH 7.4; (---) 2 °C, Δt after mixing does not exceed 1 min; (▲) 7 °C, Δt = 3 min; (—·—) 7 °C, Δt = 7 min; (—) 25 °C, Δt = 10 min. (Insert) Same experimental conditions: (×) 7 °C; (▲) 25 °C.

Table I: Absorption and CD Data for Complexes I, II, I′, and II′

com-plex	absorption λ (nm)	ε	assignment	CD λ (nm)	Δε
I			$^1A_1 \rightarrow {}^1E$	550	−0.7
	450	740	$^1A_1 \rightarrow {}^1A_2$	460	4.7
	385 (sh)	2500	$d\pi \rightarrow \pi^*_v$	400	−0.3
	340 (sh)	10000	$\pi^*_h \rightarrow d\sigma^*$	340	3.9
				305	−2.4
				262	−5.7
II	585	80	$^1A_1 \rightarrow {}^1E$	605	−0.8
	440	230	$^1A_1 \rightarrow {}^1A_2$	450	6.2
				390	−0.4
	355 (sh)	3000		350	−2.3
	330 (sh)	8500	$\pi^*_a, \pi^*_b \rightarrow d\sigma^*$	325	1.7
				290	−2.0
				262	−3.7
			$^1A_1 \rightarrow {}^1E$	535	−2.1
I′	470	800	$^1A_1 \rightarrow {}^1A_2$	460	5.7
	375 (sh)	6700	$d\pi \rightarrow \pi^*_v$	385	−1.5
	340 (sh)	14300	$\pi^*_h \rightarrow d\sigma^*$	340	6.1
				313	−9.4
II′	592	180	$^1A_1 \rightarrow {}^1E$	615	−2.1
	460	460	$^1A_1 \rightarrow {}^1A_2$	462	8.1
				400	−1.0
	355 (sh)	4250		370	−1.3
	335 (sh)	7500	$\pi^*_a, \pi^*_b \rightarrow d\sigma^*$	335	6.7
				310	−4.5

a $^1A_1 \rightarrow {}^1A_2$ transition and the one at lower energy to the $^1A_1 \rightarrow {}^1E_a$ transition. Using the method of Wentworth & Piper (1965), we estimated the in-plane crystal field strength and the low-axial field strength to be respectively 2550 and 1840 cm^{-1} for complex I and 2650 and 1620 cm^{-1} for complex II. At this stage it is interesting to compare these results to those obtained by Dabrowiak & Tsukayama (1981) on the Co(III) complex of pseudotetrapeptide A of BLM [Co(III)·2]; they determined the in-plane crystal field strength of this complex to be 2650 cm^{-1}, which compares with those obtained for complexes I and II. This strongly suggests that the in-plane ligands are the same in the three complexes, i.e., the secondary amine, N(1) of the pyrimidine, the deprotonated amide nitrogen atom of the β-hydroxyhistidine, and N(3) of the imidazole (Dabrowiak & Tsukayama 1981). The Co(III)·2 complex has the primary amine group of the peptide and a water molecule occupying the two axial positions. In complexes I and II it is very likely that the two axial positions are occupied by the primary amine group and by O_2^- and O_2^{2-}, respectively. This suggests that the crystal field strength of superoxide anion is slightly higher than the one of peroxide.

In the near-UV, complexes I and II exhibit strong absorptions. Of these, the shoulder at 385 nm, which is present in the spectrum of complex I only, can tentatively be assigned to a charge transfer transition from the $d\pi$ orbitals to the π^*_v orbital of oxygen [the notations are taken from Lever & Gray (1978)], and the band at 340 nm to a $\pi^*_h \rightarrow d\sigma^*$ charge transfer transition. In the same way, we suggest assignment of the two shoulders that appear at 330 and 350 nm in the absorption spectrum of complex II to the charge transfer transitions $\pi^*_a \rightarrow d\sigma^*$ and $\pi^*_b \rightarrow d\sigma^*$.

DNA–BLM–Co^{II} System. When the addition of Co(II) to a BLM solution is performed in the presence of DNA, a superoxo Co·BLM complex that dimerizes to a μ-peroxo Co_2·BLM is obtained. However, due to the presence of DNA, the rate of dimerization greatly decreases. Under these conditions, the type of complexes obtained depends, predominantly, on three parameters: [nucleotide]/[Co] molar ratio, time, and temperature.

[Nucleotide]/[Co] ≥ 16. When the experiments are performed at 25 °C, at [nucleotide]/[Co] ≥ 16 a superoxo Co·BLM complex is obtained. This is attested by oxygen consumption (1 mol of O_2/Co) and the appearance of a very well resolved EPR spectrum (Garnier-Suillerot et al., 1981) characteristic of the well-known O_2^--bound Co(III). The EPR

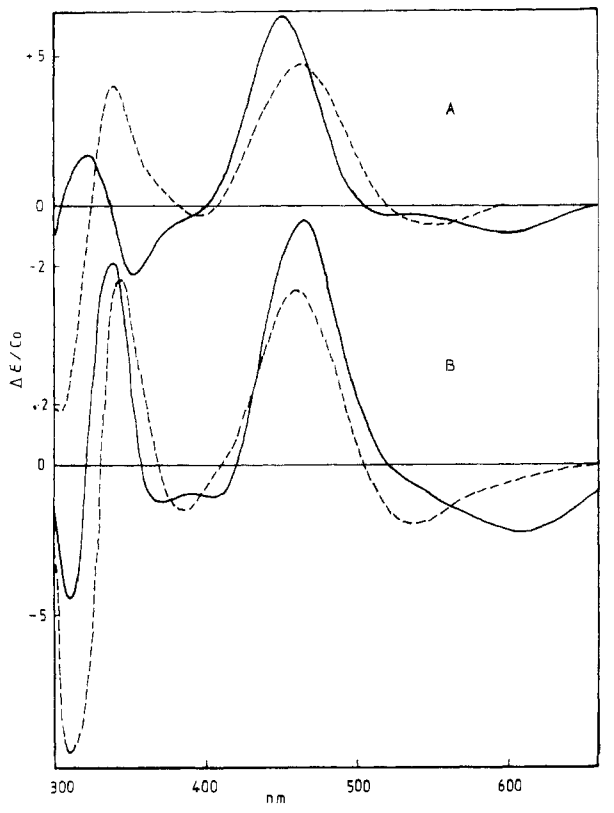

FIGURE 2: CD spectra of complexes I (--) and II (—) (curves A) and complexes I′ (--) and II′ (—) (curves B). Experimental conditions: 200 μM Co(II), 350 μM BLM in 0.01 M Hepes buffer, pH 7.4. (Curves A) (--) 2 °C, the time elapsed after mixing does not exceed 1 min; (—) 25 °C, Δt higher than 10 min. (Curves B) (--) [nucleotide]/[Co] = 16, T = 25 °C, Δt = 10 min; (—) [nucleotide]/[Co] = 16, T = 25 °C, Δt = 4 days.

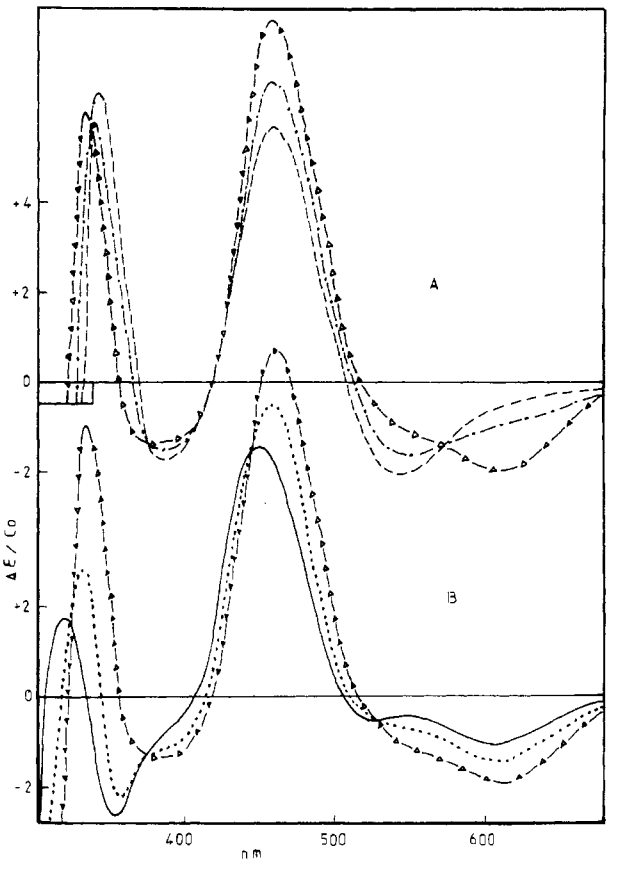

FIGURE 3: CD spectra of DNA–BLM–Co system. The spectra have been recorded 1 h after addition of Co(II) to DNA–BLM mixture at 25 °C. Experimental conditions: 200 μM Co(II), 350 μM in 0.01 M Hepes buffer, pH 7.4 [nucleotide]/[Co]: 0 (—); 2 (···); 8 (Δ); 12 (-·-); 16 (--).

parameters for this complex are as follows: $g_\perp$, 2.005; $g_\parallel$, 2.100; $A_\perp^{Co}$, 13 G; $A_\parallel^{Co}$, 20.3 G. During the following hour, neither detectable releasing of O_2 nor decreasing of the EPR signal is noticeable. Figure 2 (curve B) shows the CD spectrum of this complex, hereafter labeled I′.

Complex I′ very slowly evolves to a μ-peroxo complex, labeled II′, as the slow decrease of the EPR signal demonstrates. The CD spectra, recorded at various time intervals, exhibit isodichroic points at 575, 375, and 340 nm, indicating that only complexes I′ and II′ are present. The CD spectrum of complex II′ is shown in Figure 2 (curve B).

The rate constant of the reaction I′ → II′ has been determined at [nucleotide]/[Co] = 20. Its value at 25 °C, in Hepes buffer (0.01 M, pH 7.4) is k'_2 = 0.092 M^{-1} s^{-1}; i.e., this reaction is more than 2000 times slower than the reaction I → II. The half-time is about 18 h.

At [nucleotide]/[Co] < 16, the situation is more complex, and two differents sets of results are obtained depending on whether the [nucleotide]/[Co] molar ratio is lower or higher than 8.

8 ≲ [Nucleotide]/[Co] ≲ 16. Figure 3A exhibits the CD spectra recorded 1 h after mixing. These spectra exhibits isodichroic points at 575, 375, and 340 nm, as reported above, indicating that complexes I′ and II′ are present.

The amplitude of the EPR signal (curve a′) and the values of $\Delta\epsilon$/Co at 460 nm (curve a) are plotted in Figure 4 as a function of [nucleotide]/[Co]. As can be seen, as the molar ratio decreases from 16 to 8; $\Delta\epsilon$ at 460 nm increases from the value characteristic of complex I′ to that of complex II′. Concomitantly, the amplitude of the EPR signal evolves from that of complex I′ to zero. This means that, about 1 h after

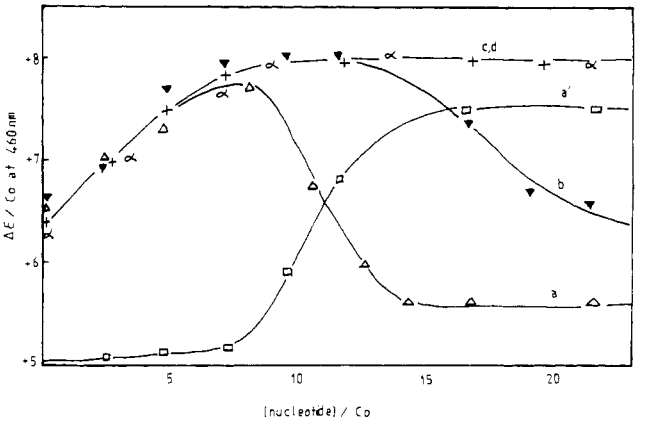

FIGURE 4: DNA–BLM–Co system: variation of $\Delta\epsilon$/[Co] at 460 nm (curves a–d) and of the EPR signal (curve a′) as a function of [nucleotide]/[Co] molar ratio. Experimental conditions: the same as those in Figure 3. Time elapsed after addition of Co(II) to DNA–BLM mixture: 1 h (curves a and a′); 20 h (curve b); 4 days (curve c). (Curve d) Complex II has been added to DNA.

mixing, at [nucleotide]/[Co] ≃ 8 only complex II′ is present, at [nucleotide]/[Co] ≳ 16 only complex I′ is present, and at 8 ≲ [nucleotide]/[Co] ≲ 16 a mixture of I′ and II′ is obtained.

As time elapses, complex I′ evolves to form complex II′, and at the end of the reaction (about 4 days) only complex II′ is present. This is attested by the plots of $\Delta\epsilon$/Co at 460 nm (curve c), which level off reaching the value corresponding to complex II′. At the same time, the EPR signal disappears. The plots of $\Delta\epsilon$ at 460 nm after 20 h of mixing, when complex I′ is still present, is also shown in curve b.

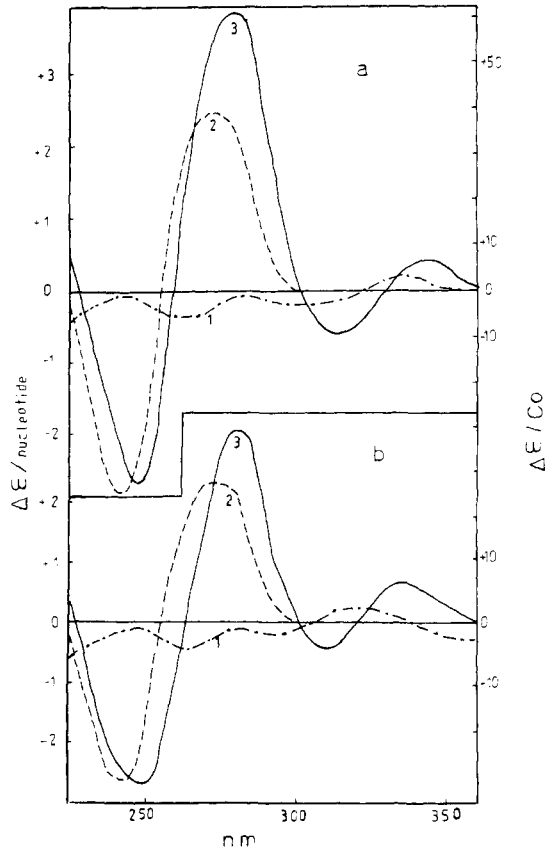

FIGURE 5: CD UV spectra of complexes I (a, curve 1) and II (b, curve 1), of DNA (a and b, curve 2), of DNA–I′ system (a, curve 3), and of DNA–II′ system (b, curve 3). Experimental conditions: [Curves 1 (a and b)] 100 μM Co(II), 160 μM BLM in 0.01 M Hepes buffer, pH 7.4; T = 2 °C, the time elapsed after mixing does not exceed 1 min (a); T = 25 °C, $\Delta t \simeq$ 10 min (b). [Curves 2 (a and b)] 10^{-3} M nucleotide in 0.01 Hepes buffer, pH 7.4, T = 25 °C. (Curves 3) 100 μM Co(II), 160 μM BLM in 0.01 M Hepes buffer, pH 7.4; [nucleotide] = 1.6×10^{-3} M, T = 25 °C, $\Delta t \simeq$ 1 h (a); [nucleotide] = 0.8×10^{-3} M, T = 25 °C, $\Delta t \simeq$ 1 h (b).

$0 \lesssim$ [*Nucleotide*]/[*Co*] $\lesssim 8$. The CD spectra recorded about 1 h after mixing exhibit isodichroic points at 530, 445, 380, and 325 nm (Figure 3B), and no EPR signal is detectable, indicating that only the species II and II′ are present. Further evolution of the equilibrium is unnoticeable at least 4 days after mixing.

DNA–Complex II System. Similar results are obtained when complex II is added to DNA. The reaction is then complete in less than 1 s at 25 °C. In this case, the spectra do not depend on the time elapsing between mixing and recording. The spectral patterns at various [nucleotide]/[Co] ratios were identical with those observed 4 days after mixing Co(II) with BLM in the presence of DNA as described above. At [nucleotide]/[Co] $\gtrsim$ 8, only complex II′ is formed (Figure 4, curve d) whereas a mixture of II and II′ is obtained at [nucleotide]/[Co] < 8 (Figure 4, curve d).

The concentrations of bound complex II to DNA (II′) and of free complex II were determined from the value of $\Delta\epsilon$ at 460 nm. The binding data were analyzed by Scatchard plots (Scatchard, 1949). A negative slope is produced in the plots of ν/c vs. ν, where ν is complex II bound per nucleotide and c is free complex II. Complex II binding to DNA appears to be a noncooperative phenomenon with an apparent equilibrium constant of 8.4×10^4 M^{-1}. One molecule of complex II binds for every 2.9 base pairs in DNA. This compares with the results obtained by Roy et al. (1981), who found that 1 Cu^{II}·BLM molecule binds for every 2.8 base pairs.

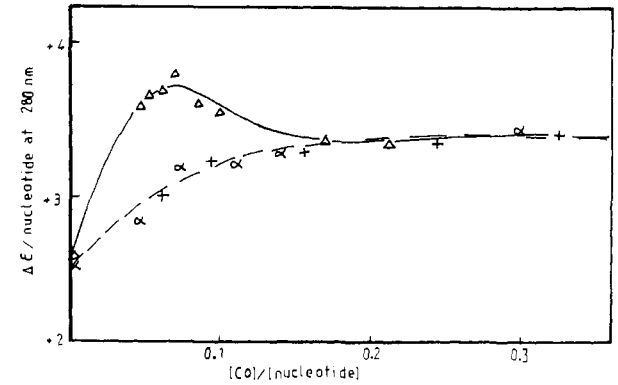

FIGURE 6: DNA–BLM–Co system. Variation of $\Delta\epsilon$/[nucleotide] at 280 nm as a function of [Co]/[nucleotide]. Experimental conditions: the same as those in Figure 3. Time elapsed after addition of Co(II) to DNA–BLM mixture: 1 h (Δ); 4 days (α). Addition of complex II to DNA (+).

Complexes I′ and II′. As can be seen in Figure 2 and in Table I, the CD spectra of complexes I′ and II′ are slightly different from those of complexes I and II. Moreover, the CD spectral pattern of DNA in the UV region displays alteration when complexes I′ and II′ are formed. The UV CD spectrum of DNA (Figure 5b, curve 2) exhibits two dichroic bands: a positive one at 275 nm and a negative one at 245 nm. The addition of complex II (curve 1) to DNA yielding complex II′ is characterized by a shift of the two bands, about 8 nm, to higher wavelengths and by an increase of the amplitude of the positive band (curve 3). Figure 6 shows the plot of $\Delta\epsilon$/[nucleotide] at 280 nm as a function of [Co]/[nucleotide]. As can be seen, there is an increase of $\Delta\epsilon$ as the molar ratio increases, and the curve reaches a plateau at [Co]/[nucleotide] $\simeq$ 0.15. Strictly analogous CD patterns are obtained when Co(II) is added to a DNA·BLM mixture and the measurements are performed approximately 4 days after mixing.

At [nucleotide]/[Co] > 8, if the data are taken 1 h after mixing, $\Delta\epsilon$/[nucleotide] at 280 nm increases steeply and reaches a maximum at [nucleotide]/[Co] $\simeq$ 16 (Figure 6). As we have shown above, the species formed at this molar ratio is complex I′. Figure 5a, curve 3, exhibits the CD UV spectrum of the DNA·I′ system thus obtained; one observes a slight shift of the two dichroic bands of DNA to higher wavelengths. For comparison, the UV CD spectrum of complex I has been plotted on the same figure (curve 1).

Two effects can account for the modifications observed in the UV CD spectrum of DNA: an overlapping of the bands of complex II′ (or I′) with those of DNA and/or modification of the bands of DNA due to conformational change. Decision making is difficult regarding the relative contribution of each effect. Nevertheless, taking into account the first effect only would led to large modification of the CD of complexes I and II through binding to DNA; for instance, the difference between spectra 3 and 2 in panels a and b of Figure 5 gives rise to a value of $\Delta\epsilon$/[Co], at 285 nm, equal to 17 for complex II′ and 32 for complex I′. These values are quite large in comparison with those of complexes I and II (Figure 5, curves 2). Therefore, it appears not irrational to suggest a modification of the CD of DNA due to conformational change. We must remind that such alterations in the CD spectral pattern of DNA have been observed upon coordination of platinum complexes to DNA bases (Macquet & Butour, 1978).

From the foregoing results, we can draw the following conclusions: (i) The superoxo complex is stabilized by binding to DNA, and about 1 molecule of complex binds for every 8 bases pairs of DNA. (ii) The Co·BLM species used clinically

to localize tumor is in fact the μ-peroxo dicobalt complex, and 1 molecule binds for every 2.9 base pairs of DNA.

Acknowledgments

We are indebted to Dr. J. Desbordes from Laboratoire Roger Bellon, who kindly supplied us with bleomycin A_2 working standard.

References

Carter, S. K. (1978) in *Bleomycin Status and New Developments* (Carter, S. K., Crooke, S. T., & Umezawa, H., Eds.) Academic Press, New York.
Dabrowiak, J. C. (1980) *Met. Ions Biol. Syst. 11*, 305.
Dabrowiak, J. C., & Tsukayama, M. (1981) *J. Am. Chem. Soc. 103*, 7543-7550.
DeRiemer, L. H., Meares, C. F., Goodwein, D. A., & Diamanti, C. I. (1979) *J. Med. Chem. 22*, 1019-1023.
Garnier-Suillerot, A., Albertini, J. P., & Tosi, L. (1981) *Biochem. Biophys. Res. Commun. 102*, 499-506.
Kakinuma, J., Kagiyama, R., & Orii, M. (1980) *Eur. J. Nucl. Med. 5*, 159-163.
Kono, A., Matsushima, Y., Kojima, M., & Maeda, T. (1977) *Chem. Pharm. Bull. 25*, 1725-1731.
Lever, A. B. P. (1968) in *Inorganic Electronic Spectroscopy*, Elsevier, Amsterdam.
Lever, A. B. P., & Gray, H. (1978) *Acc. Chem. Res. 11*, 348-355.
Macquet, J. P., & Butour, J. L. (1978) *Eur. J. Biochem. 83*, 375-387.
McLendon, G., & Martell, A. E. (1976) *Coord. Chem. Rev. 19*, 1-39.
Rao, E. A., Saryan, L. A., Antholine, W. E., & Petering, D. H. (1980) *J. Med. Chem. 23*, 1310-1318.
Rasker, J. J., Van de Poll, M. A. P. C., Beekhins, H., Woldring, M. G., & Nieweg, H. O. (1975) *J. Nucl. Med. 16*, 1058-1069.
Roy, S. N., Orr, G. A., Brewer, F., & Horwitz, S. B. (1981) *Cancer Res. 41*, 4471-4477.
Sausville, E. A., Stein, R. W., Peisach, J., & Horwitz, S. B. (1978) *Biochemistry 17*, 2746-2754.
Scatchard, G. (1949) *Ann. N.Y. Acad. Sci. 51*, 660-672.
Sugiura, Y. (1980) *J. Am. Chem. Soc. 102*, 5216-5221.
Tsukayama, N., Randall, C. R., Santillo, F. S., & Dabrowiak, J. C. (1981) *J. Am. Chem. Soc. 103*, 458-461.
Vos, C. M., Westera, G., & Van Zanten, B. (1980a) *J. Inorg. Biochem. 12*, 45-55.
Vos, C. M., Westera, G., & Schimmer, D. (1980b) *J. Inorg. Biochem. 13*, 165-177.
Wentworth, R. A. D., & Piper, T. S. (1965) *Inorg. Chem. 4*, 709-714.

Phospholipid Polar Head Group Manipulation Modulates Concanavalin A Agglutinability of LM Fibroblasts†

Friedhelm Schroeder

ABSTRACT: The effect of phospholipid polar head group manipulation in LM fibroblasts on fluoresceinylconcanavalin A binding, concanavalin A mediated hemadsorption, and concanavalin A mediated agglutination was determined. Choline analogues (*N,N*-dimethylethanolamine, *N*-methylethanolamine, and ethanolamine) were rapidly incorporated into LM plasma membrane phospholipids (35.1, 33.2, and 41.0 mol %, respectively). There were no changes in phospholipid fatty acid composition, sialic acid content, or membrane biophysical properties (characteristic break temperatures in Arrhenius plots and rotational correlation time of 1,6-diphenyl-1,3,5-hexatriene). The binding affinity of one of the two concanavalin A binding sites was doubled by all analogues tested. In addition, the concanavalin A mediated hemadsorption of sheep red blood cells and the concanavalin A mediated self-agglutinability of LM cells were doubled by choline analogue supplementation. Arrhenius plots of concanavalin A mediated agglutinability showed temperature break points for choline-fed cells at 24.3 and 33.1 °C. In contrast, *N,N*-dimethylethanolamine-, *N*-methylethanolamine-, and ethanolamine-supplemented cells had the following sets of break points: 18.3 and 27.6 °C, 10.7 and 20.1 °C, and 5.3 and 17.4 °C, respectively. The data are thus consistent with a direct correlation between lectin agglutinability characteristics and plasma membrane phospholipid polar head group composition. In addition, since the temperature break points of concanavalin A agglutinability were decreased by choline analogue supplementation while the biophysical temperature break points were not, one could hypothesize that the concanavalin A receptors may reside in specialized fluid domains within the LM plasma membrane.

Plant lectins bind to specific glycoprotein and glycolipid receptors of the cell surface. This interaction can lead to a wide variety of effects including lymphocyte stimulation (Andersson & Melchers, 1976), induction of cytotoxic effector T cells Bevan, 1976), and preferential agglutination of transformed cells (Horwitz et al., 1974; Marikovsky et al., 1974). Although the molecular basis for these effects is not well understood, several features important to lectin agglutinability of cells have emerged: plasma membrane fluidity, cell surface charge, and the cytoskeleton (McCaleb & Donner, 1981). Plasma membrane fluidity is the rate-limiting step affecting lateral diffusion of lectin receptors (Rule et al., 1979). Membrane lipids such as fatty acids, sterol/phospholipid ratio, and lysophospholipids all modulate membrane fluidity and concanavalin A agglutinability of cells (Horwitz et al., 1974; Rule et al., 1979; Rittenhouse & Fox, 1974; Hampton et al., 1980; Tombaccini et al., 1980; Ruggieri & Fallani, 1973; Bergelson & Dyatlovitskaya, 1973; Rittenhouse et al., 1974a;

† From the Department of Pharmacology, University of Missouri—Columbia, School of Medicine, Columbia, Missouri 65212. *Received May 12, 1982.* This work was supported primarily by a grant from the National Cancer Institute (CA24339) and in part by the American Heart Association, Missouri Affiliate.

0006-2960/82/0421-6782$01.25/0